ground water

Ground Water Whirls

by Kick Hemker[1], Elmer van den Berg[2], and Mark Bakker[3]

Abstract

Numerical experiments with steady-state ground water flow models show that spiraling flow lines occur in layered aquifers that have different anisotropic horizontal hydraulic conductivities in adjacent layers. Bundles of such flow lines turning in the same direction can be referred to as ground water whirls. An anisotropic layered block in a field of uniform horizontal flow results in one or more whirls with their axes in the uniform flow direction. The number of whirls depends on the number of interfaces between layers with different anisotropic properties. For flow to a well in an aquifer consisting of two anisotropic layers, with perpendicular major principal directions, whirls are found to occur in quadrants that are bounded by the principal directions of the hydraulic conductivity. The combined effect of flow to a well and a layered anisotropy implies that a single well in a system with a single anisotropic layer within an otherwise isotropic aquifer causes eight whirls. All adjacent whirls rotate in opposite directions.

Introduction

As part of a pumping test analysis in dune sands near The Hague, The Netherlands, drawdowns were measured at 12 observation wells. The observation wells were located at different distances from the pumping well in four different directions. The observed drawdowns were used to estimate the shape of the cone of depression. The shape of the cone appeared to be somewhat elliptical, which can be caused by several factors, including heterogeneity and anisotropy of the aquifer. During a discussion about the best way to proceed with the analysis, the question was raised how the flow gets affected by a single anisotropic bed within a pumped aquifer. Although there is a growing number of analytical solutions for flow to wells in layered aquifers (Maas 1987; Hemker 1999), no publications are known to the authors that discuss flow in a layered aquifer in which the anisotropic properties vary per layer. The aforementioned pumping test instigated our interest in the effects of anisotropic layers on the flow in an aquifer; the examples presented in this paper are hypothetical and have no relationship to the hydrogeologic setting of the pumping test.

The objective of this paper is to study the effects on ground water flow of homogeneous anisotropic lenses or layers within a single layered aquifer. In the absence of analytical solutions for flow in layered anisotropic aquifers, flow is simulated with a numerical model that can handle layered systems with an anisotropy that varies spatially in three dimensions. Especially the variation of the anisotropy is, in general, implemented more easily in a finite-element model. For this study, the finite-element code MicroFEM (Hemker and Nijsten 1996; Diodato 2000; Hemker 2003) was used. MicroFEM is based on a standard formulation for saturated, multiaquifer ground water flow (Freeze and Cherry 1979, Section 2.11; Verruijt 1982, Chaper 8) and can be used to construct quasi-three-dimensional multiaquifer models as well as fully three-dimensional models (Leake and Mock 1997). It also has a built-in three-dimensional particle tracker to visualize flow lines. A brief description of MicroFEM is given in the Appendix. It is important to note that the specific choice of the numerical

[1]Faculty of Earth and Life Sciences, Vrije Universiteit, De Boelelaan 1085, 1081HV Amsterdam, The Netherlands; kick.hemker@falw.vu.nl

[2]Now at Schlumberger Cambridge Research, High Cross, Madingley Rd., CB3 OEL Cambridge, UK; formerly with the faculty of Earth and Life Sciences, Vrije Universiteit, De Boelelaan 1085, 1081HV Amsterdam, The Netherlands

[3]Department of Biological and Agricultural Engineering, University of Georgia, Athens, GA 30602

Received August 2002, accepted May 2003.

model is irrelevant; the presented examples may alternatively be modeled with MODFLOW (McDonald and Harbaugh 1988) in combination with MODPATH (Pollock 1994), as long as the numerical grid is aligned with the principal directions of the hydraulic conductivity tensor.

Steady flow is considered in a simple box-shaped aquifer. The boundary conditions are chosen such that, under isotropic conditions, flow is either uniform or radial. Several configurations with one or two anisotropic beds will be considered at first without a well, later with a well present. All presented models are composed of a few relatively thick anisotropic layers to clearly demonstrate their effect on the flow. In real aquifers, layers or beds have thicknesses that usually range from 1 cm to 1 m, especially in sedimentary aquifers. Between adjacent beds, there are abrupt changes in textural and depositional conditions. Within a bed, the internal sedimentary structures, such as the type of ripple-lamination or cross-bedding, are characterized by varying dipping angles and directions because of spatial fluctuations in the depositional processes. As a result, the transmissivity of beds will often be anisotropic, while it will also vary from bed to bed in magnitude and direction.

Examples will be presented of characteristic flow patterns as they occur within and near the anisotropic beds. All flow patterns are characterized by bundles of spiraling flow lines. The three-dimensional shape of these bundles of flow lines are not easily presented in graphs. It may be beneficial to reproduce the results of the presented two-layer models and similar flow line patterns on your own computer, for example with the LT version of MicroFEM. This LT version, two finite-element models and an instruction file, are available over the Internet.

A Simple Model of Two-Layer Crosswise Anisotropy

Consider a box-shaped, two-layer, homogeneous aquifer. The model box is 200 m long, 70 m wide, and 20 m thick, and consists of two layers, each 10 m thick. The dimensions are chosen for convenience and do not affect the character of the flow field significantly, as will be shown later. An anisotropic block is located at the center of the box and is 150 m long, 20 m wide, and 20 m thick (Figure 1). The model boundaries are 25 m from the block. Inside the anisotropic block, the major principal directions of the horizontal hydraulic conductivity tensor are orthogonal. The general flow direction is lengthwise (straight north) and makes an angle of 45° with either of these directions (Figure 1). A finite-element grid is adopted with 2470 nodes and 4800 triangular elements in each layer. The nodal distances decrease from 4 m at the model boundaries to 2 m inside the anisotropic block (the finite-element grid is shown in Figure 9 in the Appendix).

The hydraulic conductivity of the isotropic outer area is 1 m/day. Within the anisotropic block, the major principal value of the horizontal hydraulic conductivity tensor is K_{max} = 1 m/day, and the minor principal value is K_{min} = 0.1 m/day, so that the anisotropy ratio is K_{max}/K_{min} = 10. The major principal directions of the horizontal hydraulic conductivity in the two layers are perpendicular to each other—southeast-northwest in the upper layer, and southwest-northeast in the lower layer; this is referred to here as crosswise anisotropy. It is noted that this combination of crosswise anisotropy and uniform flow direction is chosen because it is expected to have the greatest possible effect on the flow field; circumstances in nature are likely to be less

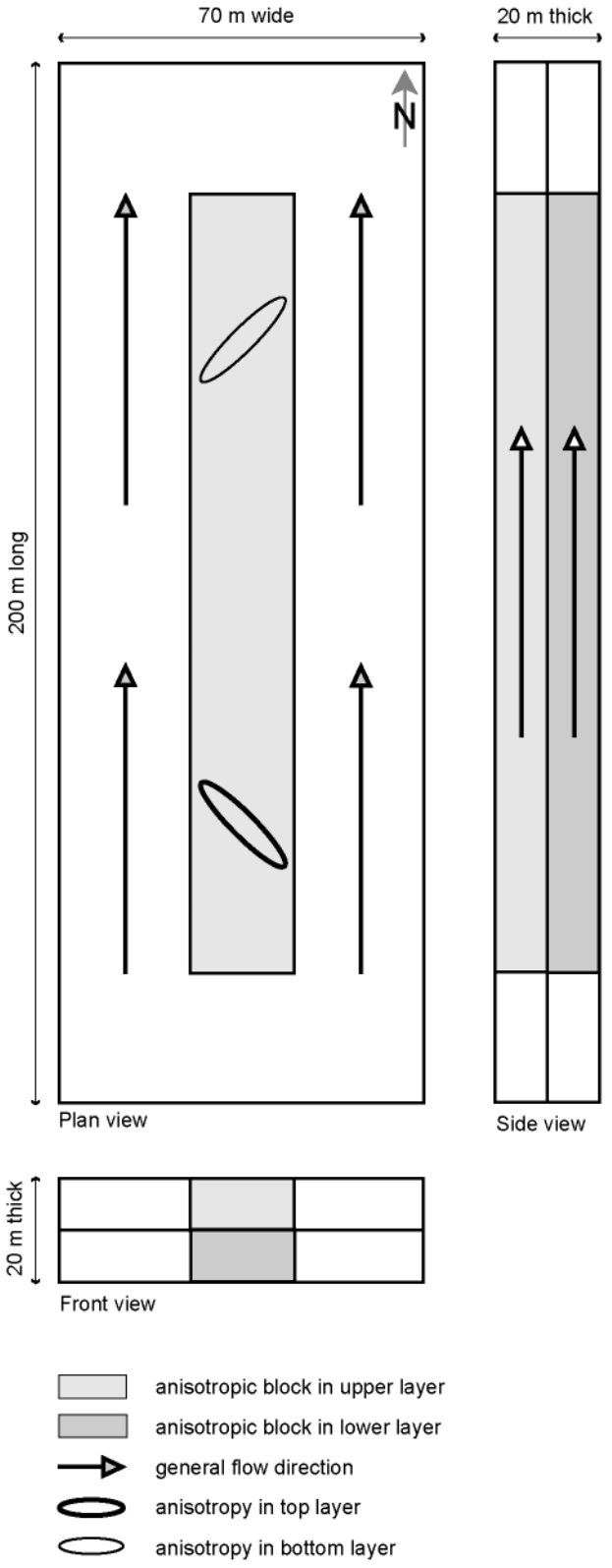

Figure 1. Plan, side, and front view of a two-layer model with crosswise anisotropy. The major principal direction of anisotropy is northwest in the upper layer and northeast in the lower layer.

extreme. In addition, the choice of a crosswise anisotropy allows for the replication of the results with a model that can only simulate crosswise anisotropy.

The vertical hydraulic conductivity in the isotropic and anisotropic parts is K_v = 1 m/day, which is modeled as a hydraulic resistance (the reciprocal of the leakance) at the interface between the two layers. The resistance represents the vertical resistance to flow between the centers of the two layers. For this case, the distance between the centers of the two layers is b = 10 m, so that the resistance is equal to c = b/K_v = 10 days. Flow in the aquifer is fully confined. The western and eastern sides are no-flow boundaries, while the short southern and northern sides are open boundaries with fixed potentiometric heads that differ by 1 m. It is noted that the specific value of the gradient has an effect on the values of the potentiometric contours and velocity only, and does not affect the pattern of potentiometric contours and flow lines.

A plan view of the model with potentiometric contours and flow lines is shown in Figure 2. The contours are drawn with an interval of 0.1 m. The maximum vertical head difference between both layers is 0.018 m. The anisotropy seems to have little effect on the contours in both layers. Small indentations are present at the boundaries of the anisotropic block, with opposite directions in the two layers. Within the anisotropic block, the contours deviate some 10° from the east-west direction, turned clockwise in the upper layer, and counterclockwise in the lower layer.

If the model would be isotropic, there is a uniform flow to the north with a total discharge of 70 m × 20 m × 1 m/day × 1/200 = 7 m^3/day. As a result of the anisotropy, the discharge is reduced to slightly less than 6.3 m^3/day. Water balance computations for each layer show that vertical flow components between both layers are induced, exchanging 3.2 m^3/day in both directions. When looking downstream, ground water flows upward in the eastern half of the model, with a maximum at the boundary of the anisotropic block. Vertical flow in the western half of the model is downward.

Five flow lines are shown in Figure 2, all starting in the upper layer at the center of the southern model boundary, at depths of 1, 3, 5, 7, and 9 m from the confined top; the flow lines are numbered 1 through 5 from top to bottom. Since MicroFEM assumes the horizontal flow components to be the same at any depth within a layer, just like in MODPATH, these flow lines remain on top of each other as long as no line crosses the interface to enter the lower layer. The vertical components of flow are computed by considering three-dimensional continuity of flow at any point in the aquifer, and are obtained by linear interpolation between the vertical flow components at the upper and lower layer boundaries (Strack 1984). In Figure 3, the same five flow lines are projected on a vertical profile, perpendicular to the north-south direction. Flow line 1, starting 1 m below the confined top, remains in the upper layer while all other flow lines run through part of the lower layer. The lower a flow line starts in the upper layer, the sooner it crosses the interface and the sooner it comes back to the interface again. The zigzag lines in Figure 2 are caused by the repeated crossings of the interface and the alternating flow directions in the two layers. Markers on the flow lines indicate a residence time interval of 10 years, based on 30% porosity. The

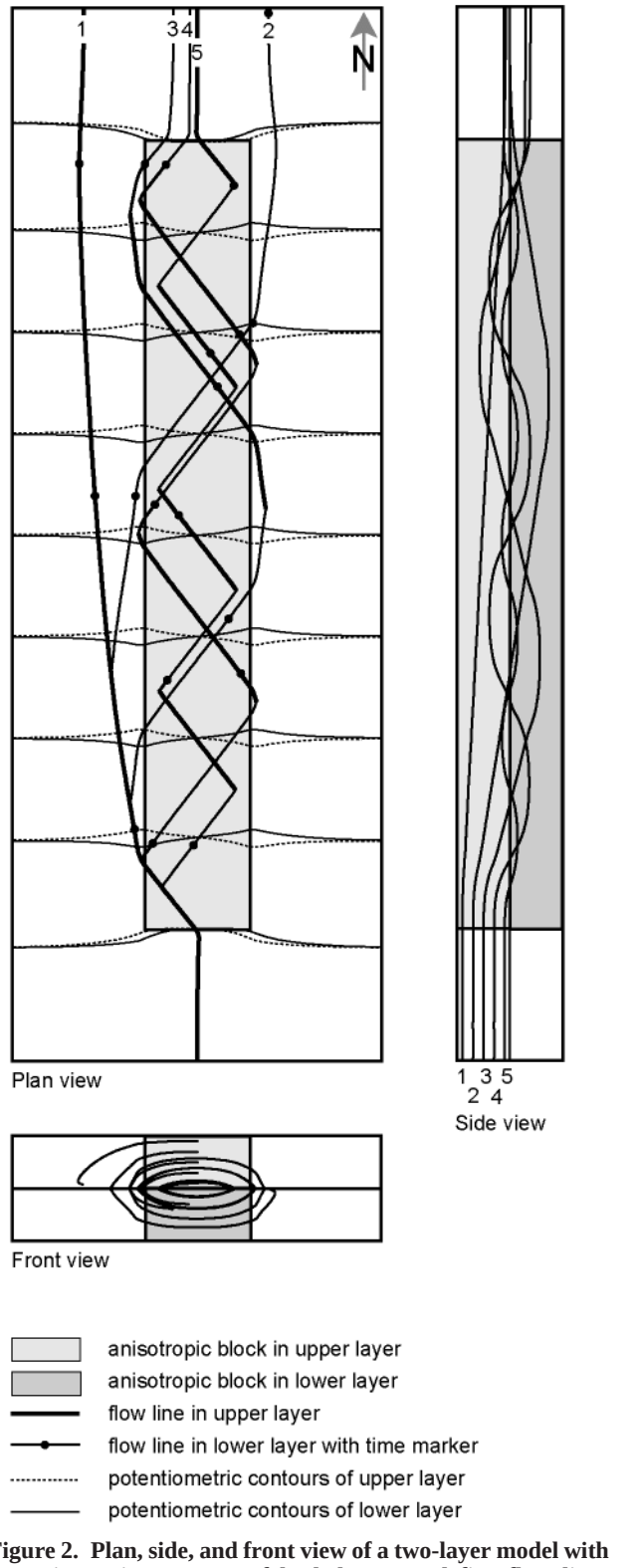

Figure 2. Plan, side, and front view of a two-layer model with potentiometric contours of both layers and five flow lines starting at different levels in the upper layer on the southern model boundary.

computed total travel times are 35.2, 40.2, 46.7, 56.6, and 57.7 years from the uppermost to the lowermost flow line, respectively.

The bundle of flow lines of Figure 3 has a number of interesting properties. Although the isotropic areas near the beginning and end of the flow field produce some distortions, it is clear from the concentric shapes in Figure 3 that

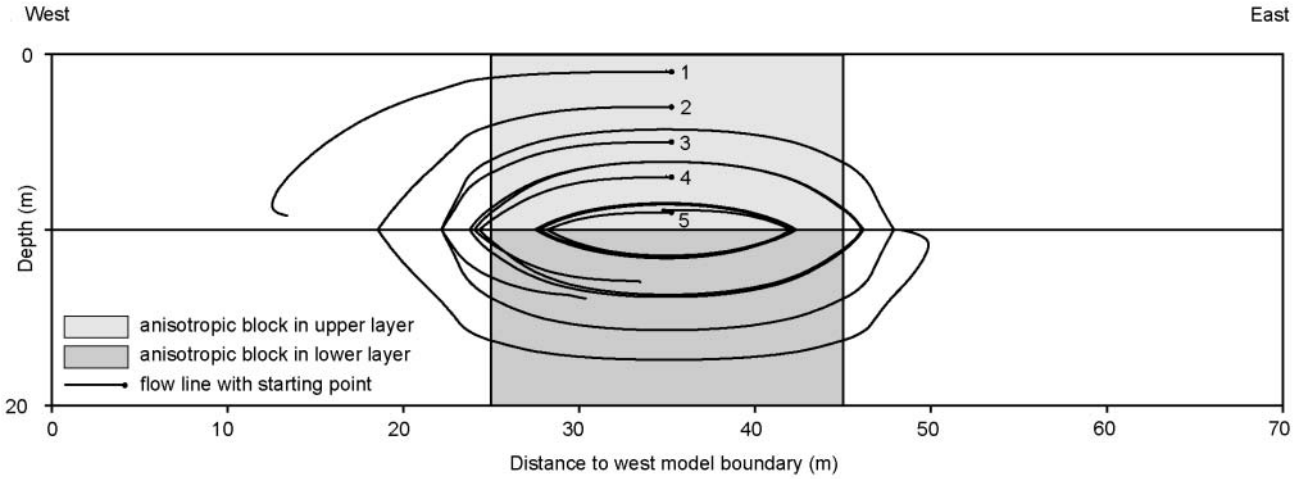

Figure 3. The five spiraling flow lines of Figure 2 projected in the general direction of flow on an east-west cross section.

each flow line that goes through the anisotropic block shows a repetition of the same three-dimensional curve. Flow lines starting close to the interface between the two layers make more revolutions than flow lines starting farther away from the interface. The bundle of spiraling flow lines turning in the same direction is termed a ground water whirl here.

Ground Water Whirls in Fields of Uniform Flow

The ground water whirl shown in Figure 3 shows sharp folds at the interface between the two anisotropic layers, as would be expected at a discontinuity in the hydraulic conductivity. Although an abrupt change in the direction of flow occurs at the interface, it is likely that the discretization of the model in just two finite-element layers increases this behavior. Other simplifications that may be responsible for the specific shape of the whirl are the no-flow model boundaries at the top and bottom of the aquifer, and the relatively short distance between the anisotropic block and the western and eastern no-flow boundaries.

To analyze the effects of the vertical discretization as well as of the top and bottom boundary conditions, a model was constructed with 20 finite-element layers each 1 m thick. The anisotropic block is chosen at the center of the model and is 10 m wide and 10 m high. The top half of the anisotropic block has an anisotropy equal to the upper layer of Figure 1, the bottom half has an anisotropy equal to the lower layer of Figure 1. The five finite-element layers at the top and bottom of the aquifer are isotropic. The values of the aquifer parameters were chosen identical to the previously described two-layer model. As a result of the finer vertical discretization, flow lines have a more rounded shape when looking in the general flow direction (Figure 4). Note that without the anisotropic layers, the projection of flow lines would appear as dots. As a result of the new configuration, additional clockwise whirls develop near the top and near the bottom of the anisotropic block, above and below the anticlockwise whirl around the central axis of the block. The axes of the upper and lower whirls are located along the centerlines of the top and bottom boundaries of the anisotropic block. Apparently, whirls will appear near any level where a change of anisotropy occurs with depth, including a transition from isotropic to anisotropic conditions. These upper and lower whirls, however, are not rotating symmetrically around their axes. In a cross section, the flow components are relatively large in a narrow zone at the

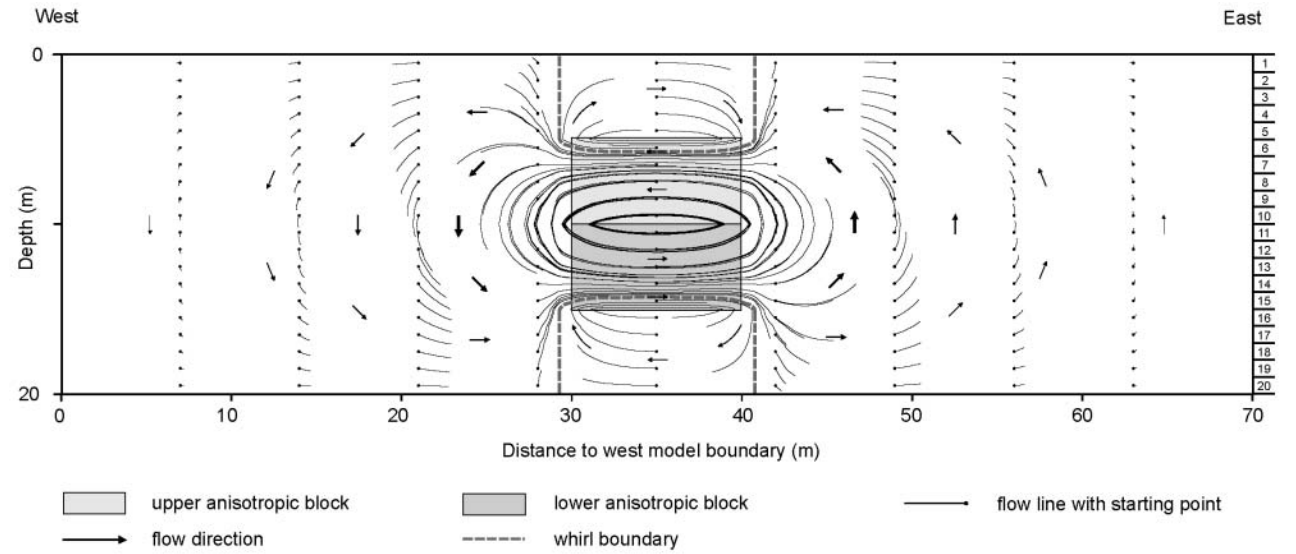

Figure 4. Cross section showing projected flow lines to identify one symmetric and two asymmetric whirls caused by crosswise anisotropy of a block in the center of the aquifer.

top and bottom of the anisotropic block next to the central whirl, while this flow component is small and more diffuse in the outer, isotropic part.

To reduce the possible interference of nearby model boundaries even further, the aquifer box was increased to 1000 m long, 1000 m wide, and 241 m thick. One anisotropic layer is present at the center and is 200 m long, 20 m wide, and 1 m thick. The anisotropic layer is represented by one finite-element layer; adjacent layers above and below are 3, 9, 27, and 81 m thick, increasing away from the center of the aquifer. Again, the maximum and minimum hydraulic conductivities are 1 m/day and 0.1 m/day respectively, with a major principal anisotropy direction (southeast-northwest) that deviates 45° from the general flow direction (north). In agreement with the previous 20-layer model, two asymmetric whirls occur, turning in opposite directions. The symmetric whirl of the previous example is absent, since there is only one anisotropic layer. Anisotropy has practically no effects on the hydraulic heads in the thin middle layer; flow is driven here nearly in the major principal direction, which causes the asymmetric whirls above and below the anisotropic layer. This effect is quantified in Figure 5, where a large number of south-north running flow lines of exactly 100 m long are projected on a west-east cross section. The projections of the flow lines give a clear view of the whirling flow properties near the anisotropic layer**.** At the east side, flow converges and flows into the thin anisotropic layer, while on the west side, flow diverges and contributes to both whirls. From the length of their projected parts, it follows that, for this case, the effect of the ground water whirl is only significant in a zone of ~20 m around the anisotropic layer.

Flow to a Well with Four Whirls

The two-layer model with crosswise anisotropy of Figure 1 produced the simplest results, with only one ground water whirl. A similar setup will be used to study the effects of layered anisotropy on flow to a well, with the anisotropic properties chosen to extend over the entire model area. A square model of 1000 m × 1000 m is considered with a fully penetrating well at the center of the confined aquifer. The model consists of two anisotropic layers, each 10 m thick. The maximum horizontal conductivity is 1 m/day, the anisotropy ratio is 10, and the major principal directions are perpendicular to each other—northeast in the upper layer and northwest in the lower layer. The vertical hydraulic conductivity is 1 m/day, which is modeled as a hydraulic resistance of 10 days (a leakance of 0.1/day). Along the model boundary, the heads are fixed at 0 m; the well pumps 100 m^3/day, equally divided over both layers. The nodal distances of the finite-element grid decrease gradually from 100 m at the boundary to 1 m near the well for a total of 681 nodes per layer.

The resulting cone of depression is nearly circular with practically the same drawdowns in both layers, except for a relatively small area around the well (Figure 6). Away from the well, the average drawdown $(s_{upper} + s_{lower})/2$ approaches the drawdown computed for an isotropic aquifer if the horizontal hydraulic conductivity is set to $(K_{max} + K_{min})/2$. The relative difference in drawdowns between the two anisotropic layers is < 4% outside a circle with a radius of 30 m from the well. Within this radius, the shape of the drawdown contours is elliptical, oriented in the major principal directions of the anisotropy (Figure 6). This radius agrees well with the characteristic length at which vertical head differences become negligible, often defined as three or four times the leakage factor of leaky aquifers (Verruijt 1982, p. 22). This radius is actually the same as the radius of influence of partial penetration in a vertically anisotropic aquifer of thickness B (Hantush 1964, p. 351; Bear 1979, p. 344), which is defined as 1.5 or $2B\sqrt{K_h/K_v}$, depending on the adopted approximation. When replacing K_h by $(K_{max} + K_{min})/2$, a distance of 22 or 30 m is obtained.

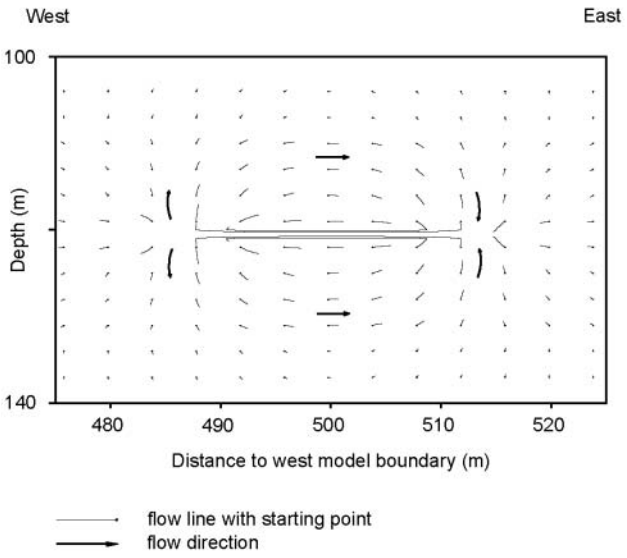

Figure 5. Cross section showing projected flow lines to identify two asymmetric whirls caused by a single, thin anisotropic layer in the center of a thick aquifer.

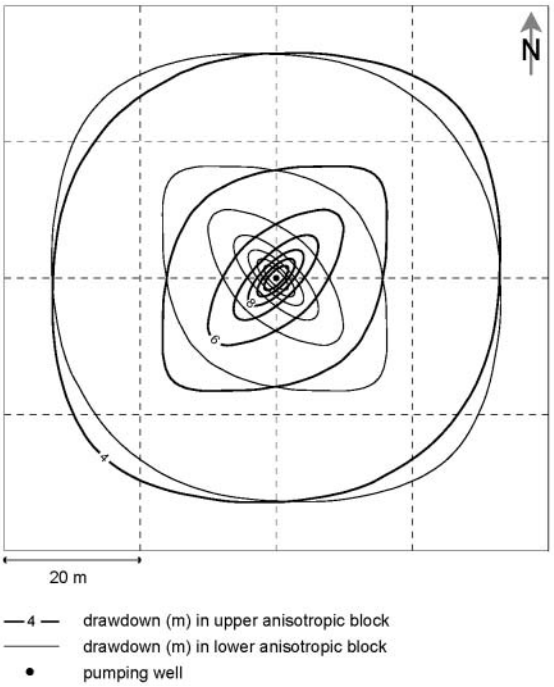

Figure 6. Drawdown contours around a well in the upper and lower layer of a two-layer aquifer with crosswise anisotropy.

Water balance computations show that the vertical exchange between the two layers is ~100 m^3/day upward and the same amount downward for the area within a range of 350 m from the well. By comparing these vertical flow components to the well discharge for each layer (50 m^3/day) and the boundary inflow (also 50 m^3/day for each layer), it means that on average a flow line passes the interface twice upward and twice downward within this range of 350 m from the well.

Analysis of flow line patterns shows there are four whirls present in the flow system (Figures 7 and 8). The presence of these whirls can be directly derived from the

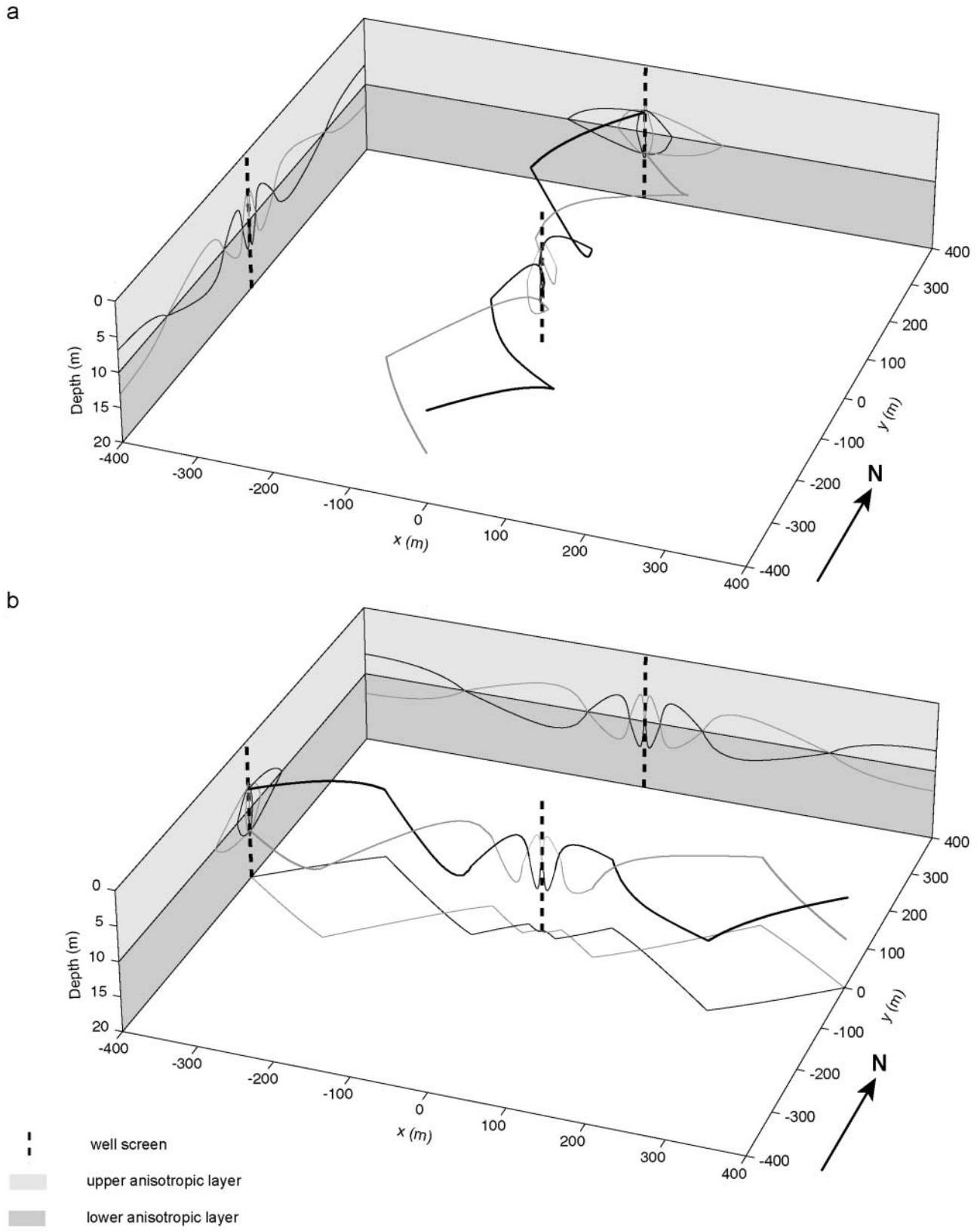

Figure 7. Three-dimensional representations of flow lines near a well in a two-layer aquifer with crosswise anisotropy, with vertical and horizontal projections: (a) two flow lines starting from straight south and two from straight north, and (b) two flow lines from straight east and two from straight west.

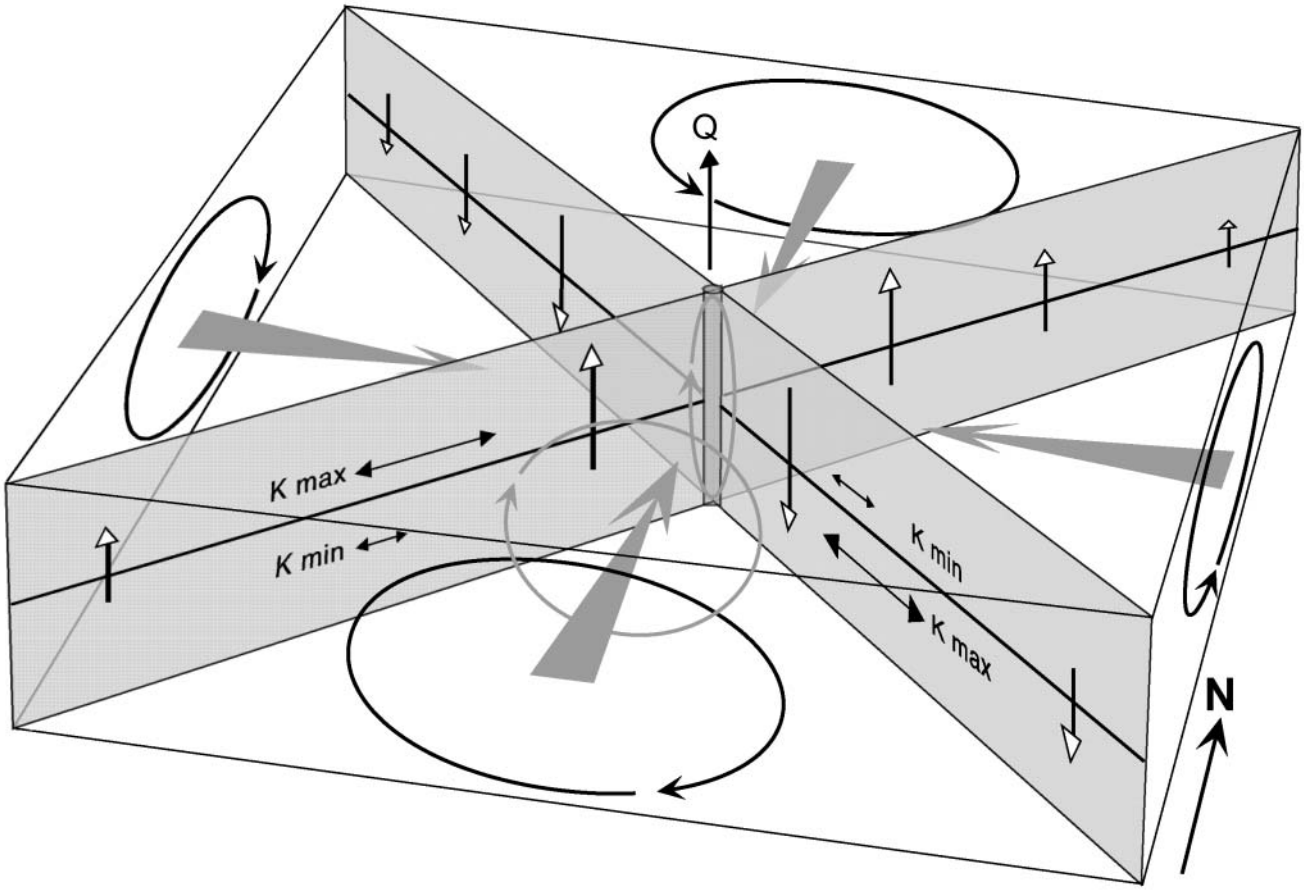

Figure 8. Schematic representation of four whirls induced by flow to a well in a two-layer aquifer with crosswise anisotropy.

two elliptical drawdown cones in Figure 6. From inspection of the potentiometric contours, it becomes clear there are four radial directions along which horizontal flow is radial in both layers; these radial directions correspond with the southwest-northeast and northwest-southeast directions, i.e., the principal directions. These radial directions represent two vertical planes that intersect at the well. In the southwest-northeast vertical plane, the vertical flow components are upward. In the northwest-southeast plane, the vertical flow is downward (Figure 8). The whirls are bounded by the quadrants as defined by these planes (Figure 8). While flow approaches the well, the changing height-width ratio of the quadrants shapes the whirl—away from the well the whirl is wider than it is tall; near the well screen it is taller than it is wide (Figure 7). It is noted that the same reasoning applies when the major principal directions of the hydraulic conductivity tensors are not orthogonal. In that case, the angle between the main axes of the elliptical head contours will be smaller than 90°, but there will still be four whirls. Adjacent whirls rotate in opposite directions.

The knowledge gained from the previous examples may be applied to determine the characteristics of the originally posed problem of flow to a well in an aquifer with a single anisotropic layer somewhere in the middle of an otherwise isotropic aquifer. The resulting intricate flow pattern can be explained as the combined effects of previously discussed flow systems. Every quadrant now has two whirls, one above the other (as in Figure 5). Hence, the total number of whirls is eight. Each whirl is adjacent to three others and all adjacent whirls rotate in opposite directions. The three-dimensional graphical depiction of such a flow field is complicated and not shown here, but it is similar to that of Figures 7 and 8, but now with two layers of whirls on top of each other, with adjacent whirls rotating in opposite directions.

Discussion

Several different flow patterns were presented for flow in layered aquifers with different anisotropic, horizontal hydraulic conductivities. It was shown that bundles of spiraling flow lines, referred to as ground water whirls, occur near vertical discontinuities in the anisotropy. This conclusion was based on several simple settings consisting of a few layers with different anisotropy properties. The aquifer parameters were fixed; the major principal directions of the anisotropy in different layers were perpendicular, the anisotropy ratio was 10, and the vertical hydraulic conductivity was equal to the maximum horizontal conductivity. Other combinations of anisotropy ratios and angles between major principal directions, as well as more anisotropic layers, will result in an infinite number of similar flow patterns. All presented numerical models simulated the effects on the flow pattern of changing anisotropy properties in the vertical direction only. Lateral transitions were not considered, but such conditions can be modeled just as easily. An anticlockwise whirl may immediately turn into a clockwise

whirl when ground water moves laterally into an area with contrasting anisotropy properties. The presented ground water whirls near wells were confirmed recently by an analytical theory based on the Dupuit approximation (Bakker and Hemker 2002); this paper shows whirls near wells in aquifers consisting of one isotropic and one anisotropic layer.

From a practical point of view, it should be realized that it will not be easy to detect ground water whirls in the field. The accompanying vertical head differences are generally small and may be smaller than head differences caused by local heterogeneity. Nevertheless, whirls may play an important role where the mixing of water is concerned in general, and the spreading of contaminant plumes in particular. Since transport models often disregard anisotropic properties that vary per layer, the effect of whirls will show up during calibration as a relatively large mechanical dispersion. In this respect, it is stressed that whirls are, by definition, three-dimensional flow phenomena that can never be simulated with two-dimensional models.

In this paper, it was shown that anisotropy in nonhomogeneous models leads to ground water whirls. This phenomenon can play a role at any scale. All that is required is a nonhomogeneous anisotropic matrix. It was not the purpose of this paper to demonstrate the existence of anisotropy in reality. Unless one believes that all layers (beds) are always isotropic, ground water whirls will exist. It is noted, however, that the whirls we presented with our simple models were the result of a rather extreme contrast in anisotropy between layers. This extreme contrast was chosen to maximize the effect on the flow of anisotropy in nonhomogeneous models; the contrast is likely to be less extreme in nature.

The presented flow patterns were mainly illustrated with two-dimensional figures of complicated three-dimensional flow patterns. The graphs were kept simple, since complex patterns are hard to interpret. It is, however, much more informative to generate these flow patterns on a computer screen, thus allowing for different projections, zooming, and colors. The flow patterns for the models with two finite-element layers, and other two-layer models, may be generated with the LT version of MicroFEM, which is available for free over the Internet.

Acknowledgments

The authors thank Otto Strack, Clifford Voss, and four anonymous reviewers for their comments and suggestions, and Gualbert Oude Essink for demonstrating ground water whirls in a MODFLOW model.

Editor's Note: The use of brand names in peer-reviewed papers is for identification purposes only, and does not constitute endorsement by the authors, their employers, or the National Ground Water Association.

References

Bakker, M., and K. Hemker. 2002. A Dupuit formulation for flow in layered anisotropic aquifers. *Advances in Water Resources* 25, 747–754.

Bear, J. 1979. *Hydraulics of Groundwater*. New York: McGraw-Hill.

Diodato, D.M. 2000. Software Spotlight: MicroFEM Version 3.50. *Ground Water* 38, no. 5: 649–650.

Freeze, R.A., and J.A. Cherry. 1979. *Groundwater*. Englewood Cliffs, New Jersey: Prentice-Hall.

Hantush, M.S. 1964. Hydraulics of wells. In *Advances in Hydroscience*, vol. 1, ed. V.T. Chow, 281–432. New York: Academic Press.

Hemker, C.J. 1999. Transient well flow in layered aquifer systems: The uniform well-face drawdown solution. *Journal of Hydrology* 225, 19–44.

Hemker, C.J. 2003. Internet site. http://www.microfem.com.

Hemker, C.J., and G.J. Nijsten. 1996. *Groundwater Flow Modeling Using MicroFem: Version 3*. Amsterdam, The Netherlands; Hemker Geohydroloog Amsterdam.

Leake, S.A., and P.A. Mock. 1997. Dimensionality of ground water flow models. *Ground Water* 35, no. 6: 930.

Maas, C. 1987. Groundwater flow to a well in a layered porous medium, 1: Steady flow. *Water Resouces Research* 23, no. 8: 1675–1681.

McDonald, M.G., and A.W. Harbaugh. 1988. A modular three-dimensional finite-difference ground-water flow model. U.S. Geological Survey Techniques of Water-Resources Investigations, Book 6, Chapter A1.

Pollock, D.W. 1994. User's guide for MODPATH/MODPATH-PLOT, version 3: A particle tracking post-processing package for MODFLOW, the U.S. Geological Survey finite-difference ground-water flow mode. U.S. Geological Survey Open-File Report 94–464.

Strack, O.D.L. 1984. Three-dimensional streamlines in Dupuit-Forchheimer models. *Water Resources Research*. 20, no. 7: 812–822.

Verruijt, A. 1982. *Theory of Groundwater Flow*, 2nd edition. London: Macmillan.

Appendix: A Brief Discussion of MicroFEM

MicroFEM is a Windows-based program to model steady-state and transient multiaquifer flow. It employs a two-dimensional triangular finite-element method for the lateral flow components (Figure 9) and a one-dimensional finite-difference method for vertical flow components. Confined, phreatic, and leaky multiaquifer systems can be simulated with a maximum of 20 aquifers or layers. The maximum number of nodes per layer is 50,000. MicroFEM supports heterogeneity and anisotropy that changes spatially throughout the domain. A different horizontal hydraulic conductivity, horizontal anisotropy ratio, principal direction, and vertical hydraulic conductivity may be specified for each nodal area. It uses various modes for the generation of a mesh, model setup, input editing, equation solving, postprocessing, graphical visualization, and plotting. Postprocessing includes the display of transient contour lines, velocity vectors, flow lines in two or three dimensions (particle tracking), water balances for any region, head-profiles, cross sections, and time series of heads and fluxes.

In a MicroFEM model, three-dimensional flow lines can be started from any node and from any depth. The computed lines are plotted in a map view and can subsequently be analyzed when projected onto any vertical cross section from within a specified bandwidth. In this way, there are an infinite number of possibilities to present bundles of flow lines in graphs. By experimenting with various selections

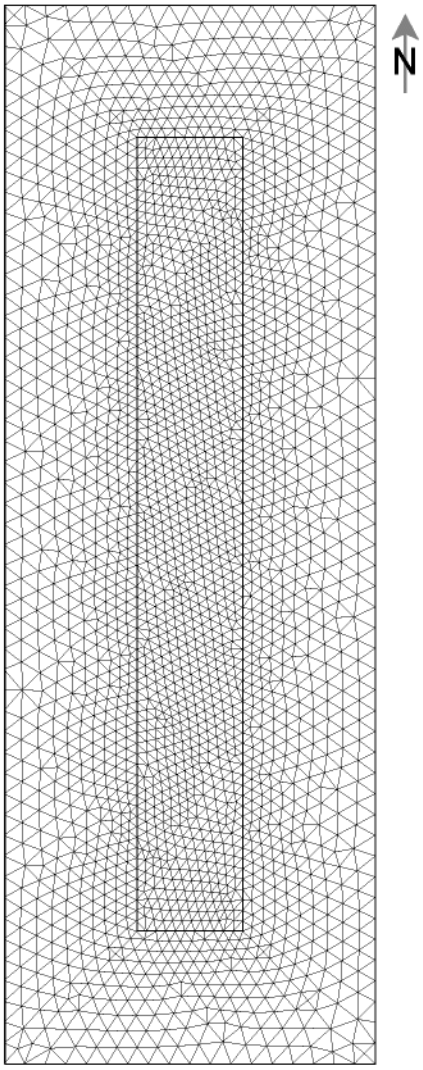

Figure 9. Finite-element grid of 2470 nodes and 4800 triangular elements, used to simulate the two-layer problem presented in Figures 1 and 2.

and with the help of the different map and profile views, entangled three-dimensional flow patterns can be analyzed.

The MicroFEM code is well benchmarked against existing software codes and published solutions. A document is available from the Internet that compares MicroFEM to analytical and MODFLOW results for a set of nine classic ground water simulations. MicroFEM is the most widely used ground water modeling program in the Netherlands. Currently there are more than 350 companies, universities, and government agencies using this software in more than 30 countries worldwide.

Both the LT version of MicroFEM and a file with the models shown in Figures 2, 3, and 7 can be downloaded for free from *www.microfem.com*. Stepwise instructions are given with the models in a one-page instruction file.